Double pane windows—elastic deformations, gas thermodynamics, thermal and optical phenomena

2014 Eur. J. Phys. 35 045023

(http://iopscience.iop.org/0143-0807/35/4/045023)

IOP Publishing European Journal of Physics

Eur. J. Phys. **35** (2014) 045023 (29pp) doi:10.1088/0143-0807/35/4/045023

Double pane windows—elastic deformations, gas thermodynamics, thermal and optical phenomena

M Vollmer[1], K-P Möllmann[1] and H J Schlichting[2]

[1] Microsystem and Optical Technologies, University of Applied Sciences, Brandenburg, Germany
[2] Department of Physics, University Münster, Germany

E-mail: vollmer@fh-brandenburg.de

Received 7 March 2014, revised 29 April 2014
Accepted for publication 7 May 2014
Published 11 June 2014

Abstract

Double pane windows are common objects which can enrich physics teaching at undergraduate level at least in five different fields. First, having sealed inner spaces filled with gas, one can discuss gas law problems upon changes of pressure and/or temperature. Second, when discussing temperature differences between inside and outside, one needs to take into account the associated heat transfer mechanisms which define the pane temperatures, enclosing the gas. Third, using elastic properties of the glass, one may treat deformations of the window panes upon those changes or additional manually applied external pressure. Fourth, the reflective properties of glass combined with the pane deformations result in concave or convex mirrors, which when illuminated by the Sun, may lead to focal points on projection areas such as facing houses. Fifth, such areas receive an increased irradiance which leads to associated thermal effects. Starting from the most obvious daily life phenomenon, the fascinating caustics of reflected sunlight on streets or walls, all of these double pane window phenomena are investigated experimentally as well as theoretically.

S Online supplementary data available from stacks.iop.org/EJP/35/045023/mmedia

Keywords: optics, elastic deformations, thermodynamics, double pane window, caustics

(Some figures may appear in colour only in the online journal)

1. Introduction

Windows in houses permit looking through the building envelope, however, at least for single pane windows, this is also associated with increased thermal losses compared to the walls. In order to reduce these losses and prevent condensation on the surfaces, double pane windows have been developed a long time ago and patents have been issued already in the 1930s (e.g. [1]). Nowadays, double pane windows (also called double glazings) are standard. They usually consist of glass sheets having around 3 to 5 mm thickness each and a gap between the two panes of between 10 and 20 mm thickness. The air tight space between the two panes is usually filled with either dry air or noble gases of lower thermal conductivities such as Ar, Kr, or Xe and pressures around ambient pressure. Mostly Ar is used, since Kr or Xe are very expensive.

Double pane windows have been extensively studied in the past and we only mention a few studies on thermal properties such as heat transfer, optical properties of coatings for use in special environments or breakage upon thermal stress (e.g. [2, 3] and thesis overview [4]). In houses, such windows are usually considered to be of planar geometry, they do, however, also exist in curved geometries, e.g. in the form of curved air plane windows (e.g. [5]) such that the outer skin of the plane is smooth.

Most optical studies of 'planar' double pane windows have focused on the optical transmission and reflection with regard to heat management. Secondary effects of the reflected light such as caustics or induced thermal effects have only been reported for large glass fronts [6] and just a few German studies exist reporting observations of optical effects from individual double pane windows [7, 8].

They are due to increased use of double pane windows in recent decades which have led to an increase of observations of associated optical effects, in particular everyday life sightings of reflection images of strange and varying geometrical forms. These optical phenomena are on the one hand interesting for physics teaching regarding the underlying optical principles of reflected image formation. As everyday life experience, they fit nicely into curricula dealing with optics of curved mirrors. On the other hand, these optical reflections may also pose problems due to the respective thermal effects: the increase of irradiance in focal areas of the images was suspected to cause damage to thermal insulation of neighbouring houses (end of video clip [9]).

The present paper investigates optical reflection effects due to deviations from planar geometry of individual double pane windows in houses at undergraduate level. It first describes everyday life observations of the phenomena and how they vary with changing conditions, second, simple model experiments for easy demonstration of the effect in a classroom are presented, third a theoretical model is described to account for the observed features, fourth the occurrence of the phenomenon is related to external meteorological conditions, and fifth we discuss the measured thermal effects within the focal areas of the caustics.

2. The phenomenon

Figure 1 depicts two (of many) typical sights of the optical phenomena due to reflection from double pane windows. Features like these may often be observed whenever sunlight is reflected from windows and the reflected light is projected on nearby walls, e.g. of buildings on the opposite side of the street. The best conditions to observe the phenomena are a low shining sun and a street running perpendicularly to the direction of the sunlight, i.e. near

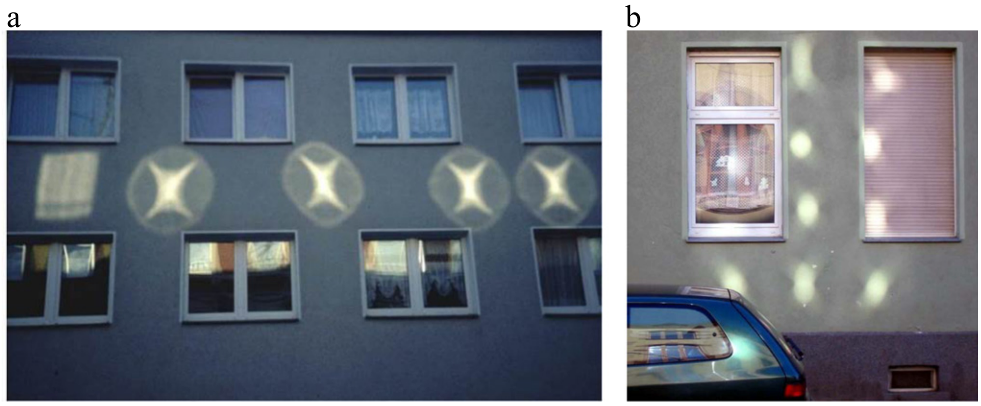

Figure 1. Two typical reflection caustics observed as projections on the walls of houses on the opposite side of the street. The geometry of the features can vary from crosses surrounded by rings or rhombuses (a) to more or less circular or elliptical shapes (b) and many more.

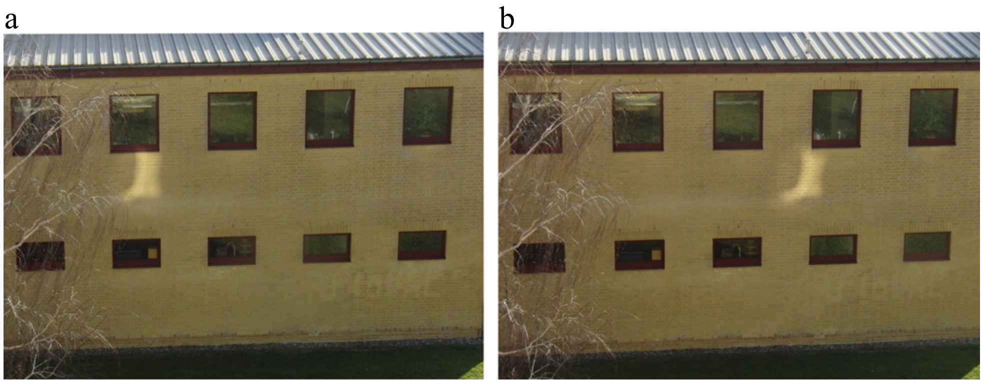

Figure 2. Two snapshots from a video of a moving caustic due to rotation of a window around its vertical axis.

normal incidence of light onto the window. When the Sun is too high the light features may eventually be found on the street or on the top of parking cars. For other geometries, the shapes from figure 1 can become quite distorted. Overall, for a given location, the phenomenon can be observed for a couple of hours each day for a period of several weeks within a given time of the year, depending on the geometry which is determined by sun path relative to building orientation.

Figure 1(a) shows a typical shape of the phenomenon, resembling a kind of light cross surrounded by a circle or rhombus of light. Such shapes are usually called caustics. Caustics refer to the enveloping curve of all light rays which were reflected by a curved window and subsequently projected onto the house wall (quite often the term caustic is used in a more general sense to describe respective focal areas when the reflected or transmitted light is projected onto a surface).

Very often, window reflections from the same house are quite similar to each other in shape (for different features, see below). In contrast the windows of adjacent houses can

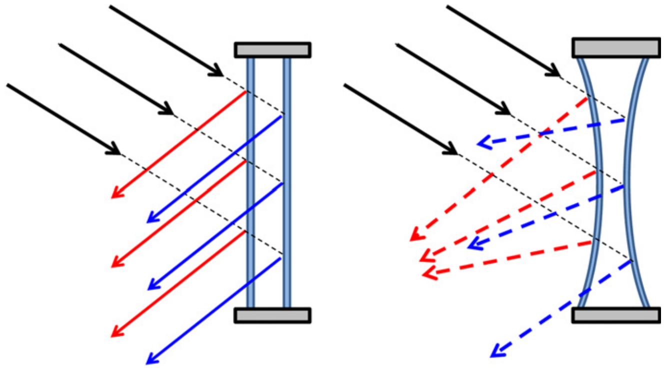

Figure 3. Scheme of a double pane window under equilibrium condition with planar surfaces (left) and if deformed (here concave shape) due to external pressure and/or temperature changes (right). The deformation can lead to focusing of light (indicated by arrows) from the front pane and defocussing from the back one (the analog situation with convex shape is also possible).

produce different reflection shapes (figure 1(b)). A rather strange observation is the fact that the sharpness of the crosses due to the same window may change within a few days leading to considerable deviations from the ideal cross shape. Also, if the projection wall distance changes, it may well be that the same window results in crosses (figure 1(a)) for nearby projection and round spots (figure 1(b)) for more distant projection.

Usually, the windows causing the phenomenon can be easily identified, e.g. by trying to look towards the reflecting windows. Alternatively as shown in figure 2, the reflecting windows are sometimes accessible. In figure 2, the window was opened and rotated around its vertical axis while recording the photos (see online supplementary data available from stacks.iop.org/EJP/35/045023/mmedia). From close-by the windows look perfectly flat, i.e. if the phenomena are due to curvatures, these must be very small.

Typical distances between windows and the projected caustics are between 10 m (figure 1) to more than 30 m (figure 2), depending on the geometry under study.

3. Simple explanation based on observations

Once it is obvious that the observed caustics result from reflection of light from windows one may either directly study the windows or—if not accessible—analyze the phenomena theoretically and/or in laboratory experiments to gain further insight in their origin. Single pane windows are rather flat and do usually not produce these caustics. Mostly double pane windows are involved.

3.1. Change of planar window panes into curved mirrors

As mentioned above, double pane windows consist of two glass panes which are separated by a volume filled with inert gas. Since the inner volume is air tight, the two glass panes are only parallel (i.e. the inner volume stays constant) if the ratio of outside pressure and temperature stays constant with respect to the manufacturing conditions of the window. Whenever this ratio changes, the inner pressure and hence, also the volume will change according to the

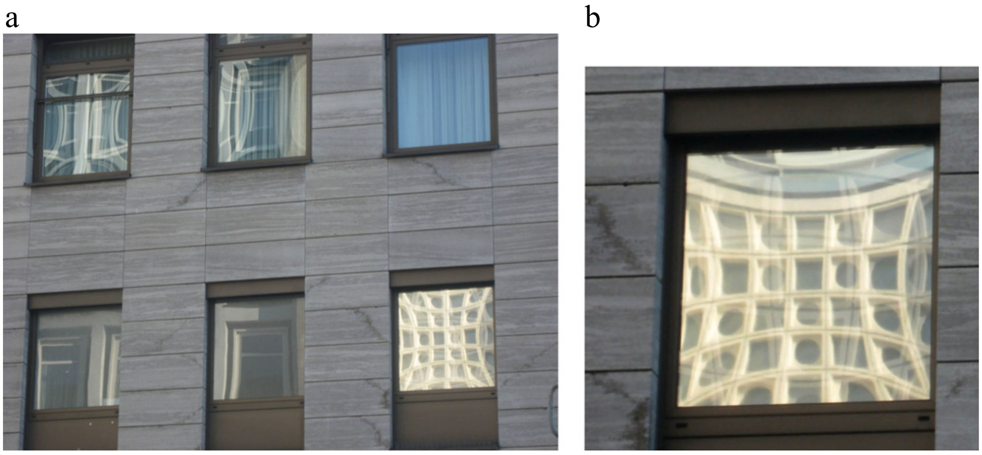

Figure 4. (a) Mirror images from rectangular structures seen in non-planar double pane windows. (b) Enlarged view of the lower right window with the distorted image nicely illustrating the window deformations.

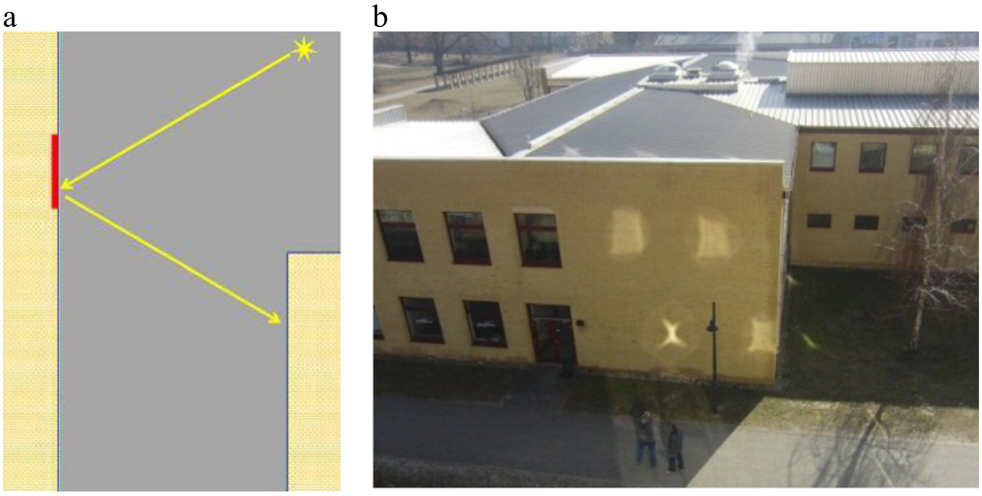

Figure 5. Geometry for observing window reflections of sunlight on buildings (a) and example of observed caustics on the wall of a neighbour building (b) (details, see text).

elasticity of the glass panes. This can lead either to convex or concave surfaces of the window, i.e. the initially planar window can change into a non-planar geometry (see figure 3).

If sunlight is incident on such a window pane with concave shape, the reflected light from the front surface of the concavely formed outside pane (figure 3) is focused. At the same time the convexly shaped inside pane leads to diverging light. Deformation of window panes can often be directly detected, when observing reflection images of rectangular objects. Figure 4 depicts an example, where deformed windows reflect other windows from houses on the opposite side of the street as well as a rectangular grid structure.

Since window panes are usually attached to a rectangular frame, the deformation will not be spherical but much more complex. For example one may expect a superposition of two

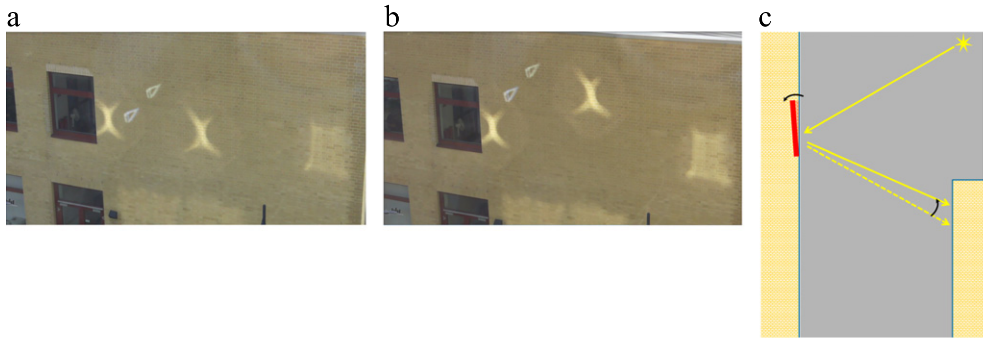

Figure 6. Moving caustic shape due to tilting of a window, i.e. rotation around a horizontal axis ((a) and (b)) as well as geometry causing the shift (c) (the two images are snapshots from a video) (see online supplementary data stacks.iop.org/EJP/35/045023/mmedia). Pane area 1.25 m × 1.74 m = 2.18 m^2.

radii of curvature and therefore the resulting focal point image will be distorted [7] from a single spot to a cross-like feature. As a first approximation we assume a spherical mirror. Its radius of curvature R defines the focal length f which in turn can be used to construct images using simple geometrical optics (see e.g. [10]). A concave spherical mirror will focus parallel (paraxial) light in a distance of $f = R/2$. In our case this means that sharp focal areas are expected whenever the image distance if close to the focal length.

In order to test the simple model of pane deformations, we did some experiments in our university building which allows observations quite regularly. Figure 5(a) shows the geometry: sun radiation is incident on a well-defined double pane window on the third floor. The reflected light is projected onto the wall of a two story neighbouring building (figure 5(b)). The direct distance from window to wall is around 30 m. The reflections of at least four windows (size 1.25 m × 1.74 m) can be seen at the nearby wall each of them being distorted differently. One of them, just observed closely by two people shows a rather sharp feature, i.e. its radius of curvature just gives a rather pronounced sharp focal spot at the projection wall of the building. For the other three windows, one of them also being at the third and the two other at the fourth floor of the office building, the image distance did not fit properly to the radius of curvature therefore the features are broader. Obviously, windows in the same building can differ appreciably from each other!

3.2. Identifying the window

First, we did identify the windows by tilting one of them. Figure 6 shows an example and depicts the geometry. By tilting the window by a few degrees, the caustic moved more than 1 m upward (see online supplementary data stacks.iop.org/EJP/35/045023/mmedia). The two triangular-like structures in the image are an artefact due to reflections from the clothes of the person, who is tilting the window.

3.3. Applying pressure to window pane

Once the window referring to a specific caustic is identified, one may change the inside pressure conditions, by applying a force to the window (just manually pushing against the center of one pane) (see online supplementary data stacks.iop.org/EJP/35/045023/mmedia). Figure 7 depicts some enlarged sections of the caustics similar to the ones in figure 5(b)

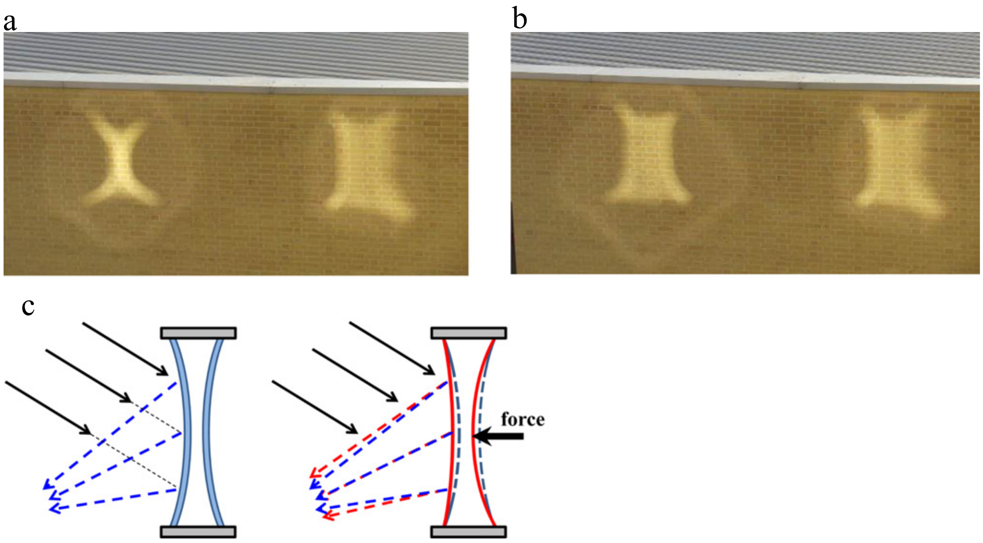

Figure 7. Change of the observed caustic of a double pane window (a) by applying a force at the inside pane (b); the geometry of figure 5 applies. Scheme of the window (c): the radius of curvature of the opposite pane changes and hence the focal area of reflected light from that pane at a given distance smears out. For simplicity, the right scheme depicts the panes as thin broken (undisturbed) or solid lines and reflection from the back pane is not shown (see online supplementary data stacks.iop.org/EJP/35/045023/mmedia).

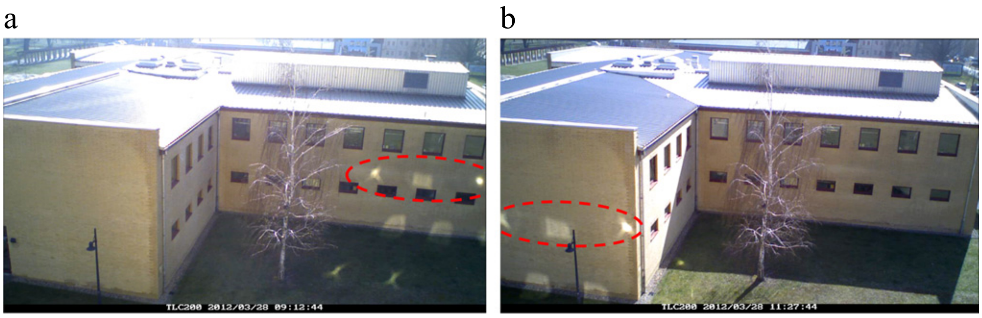

Figure 8. Two snapshots (start and 135 min later) from a time lapse video of the moving reflection features on the wall of a nearby building. The features change with image distance. Recorded 28 March 2012 (see online supplementary data stacks.iop.org/EJP/35/045023/mmedia).

before and while applying pressure. Figure 7 demonstrates that applying a force to the inside of a double pane window changes its inside pressure and therefore the geometry of the outside pane. The resulting deformations of that pane decrease or increase its radius of curvature, and the originally in focus image without force changes into an out of focus projection on the wall while applying the force. This experiment qualitatively demonstrates that it is indeed the surface geometry of the window which is responsible for the observed features.

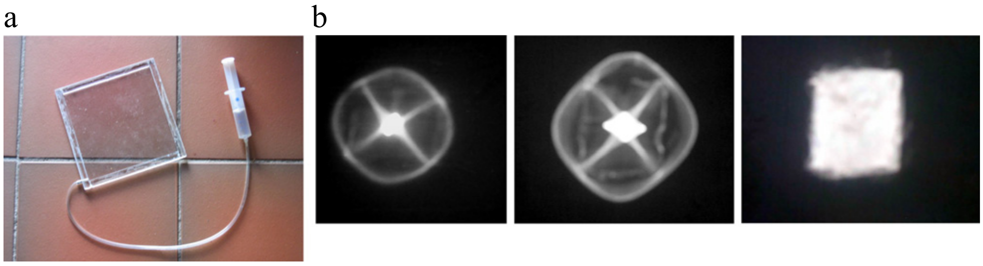

Figure 9. (a) Simple double pane window model allowing variation of the inside pressure. (b) Corresponding patterns of reflected parallel light. Left in focal distance. Middle in intermediate. Right in equilibrium.

Figure 10. Second window model (a) for quantitative measurements of plane deformation and pressure differences with two connectors to the inside volume. One connector is usually attached to a pressure and vacuum pump (b) while a coloured water manometer may be attached to the other. Besides there is the readout box of the inductive position sensor from the center of the plate (c).

3.4. Changing the image distance

A second parameter which can be changed during observations can be the image distance while the caustics move.

Figure 8 demonstrates how features change with image distance. While the reflection spots were moving within the observed period (more than two hours, time lapse video, see online supplementary data stacks.iop.org/EJP/35/045023/mmedia) the shape of the spots changed. The left cross-shaped spot within the marked area of figure 8(a) was getting out of focus for the nearer wall (figure 8(b)) while at the same time, the near circular right focal spot obviously increased in size and changed its form into a cross-shaped feature on the nearer wall (figure 8(b)).

These changes are again consistent with the simple model: for large image distances (figure 8(a)), the right spot seems to be about in focus. This means that it needs to be out of focus when decreasing the image distance by about 12.5 m as shown in figure 8(b).

4. Simple experiments in the classroom

In order to demonstrate the phenomenon in the classroom we used two slightly different miniature models of double pane windows. Figure 9(a) depicts the simpler model for

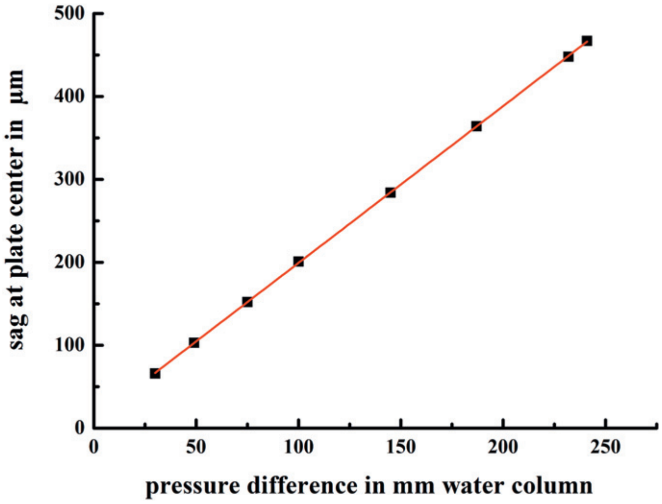

Figure 11. Sag at the center of the quadratic acryl glass plate (side length 20 cm, inner gap at equilibrium 5 mm, individual pane thickness 3.5 mm) as a function of the water column. Pressure can be calculated therefrom with the approximation that the 10 mm water column resembles approximately 1 hPa (from ρ g $h = \Delta p$).

qualitative experiments made from acrylic glass (Plexiglass). The glass sheets had a thickness of 4 mm and a size of 20 cm by 20 cm. A gap of several mm width was realized with distance pieces of the same material when gluing the glass sheets together (acrylic glass is glued together using solvent adhesives like in our case Acrifix 107 from Evonic industries: the contact surfaces are etched by the solvent and then stick together by cohesive forces while the solvent evaporates, i.e. the connection is not elastic). The inside pressure can be changed using a syringe which is attached to a nipple connector within the gap with a hose.

If the syringe is initially in a middle position, the pressure can be increased as well as decreased which—as a consequence—leads to non-planar deformations of the panes. Similar to the natural observations this is detected optically by observing reflected parallel incident light from either the Sun or a slide projector etc. Figure 9(b) depicts some experimental results for different distances of pane from projection screen.

Figure 10 depicts the second model used for quantitative measurements of window deformation due to pressure differences also made from acrylic glass. The sheets had a thickness of 3.5 mm, the inner gap was 5 mm and the window had again a size of 20 cm by 20 cm.

The inside pressure was changed with the manual pump both to larger and smaller values. It was measured using the second connector and a water manometer. Similar optical reflection patterns as in figure 9 were observed while changing the pressure from about 25 hPa to equilibrium. The pattern of the latter condition resembles the more or less featureless quadratic shape projection. The pattern does not depend a lot on the sign of the pressure difference. Switching the sign, just means that the total window shape changes from concave to convex or vice versa, i.e. the window surface responsible for the convergent pattern switches from the front pane to the back pane or vice versa.

The window model also allows measurement of the sag at the center and simultaneously the pressure difference which causes it. After evacuating the window, we observed the gradual pressure increase and simultaneously measured the sag (see figure 10(c)) with an inductive position sensor. The experiment was repeated several times. Figure 11 shows eight data points together with a straight line fit, which shows nearly perfect agreement ($R^2 = 0.999\,96$). We observed maximum sags of around 0.5 mm at pressure differences of 25 hPa, only. The linear dependence is in agreement with theoretical predictions (see equation (1) below).

5. Modeling of window deformation and caustic features

5.1. Theoretical bending of windows due to load and elastic properties

A theoretical modeling of optical features due to sunlight reflection from non-planar double pane windows starts with the distortion of the window due to pressure differences between inside and outside. The basic problem is well known in the theory of elasticity and was already treated for double pane windows in order to explain ghost image phenomena [11]. For rectangular windows of dimensions a and b and thickness h, one finds equation (1) for the sag $W(x,y)$ of a plate freely supported around its perimeter as a function of its position (x,y) (see [11] or equations (10.11) and (10.41) in [12]). We assume that the induced stresses do not lead to breaking of window panes as can occur during hurricanes [13].

$$W(x, y) = \alpha \cdot \frac{a^2 b^2}{h^3} \cdot \Delta p \cdot \phi(x, y, k). \tag{1}$$

Here, $\alpha = \frac{192(1-\sigma^2)}{\pi^6 E}$ is a factor containing the elastic properties of the plate material in form of Young's modulus of elasticity E and the Poisson ratio σ, Δp denotes the pressure difference across the plate, i.e. here the difference between inside and outside pressure. The sign convention is as follows: if the outside pressure is higher, i.e. $\Delta p > 0$, the panes will be bent inwards and $W > 0$. In the opposite case, $\Delta p < 0$ leads to $W < 0$ and bending will be outwards. $k = b/a$ is the ratio of dimensions of the plate, and

$$\varphi(x, y, k = b/a) = \sum_{m>0}^{\text{odd}} \sum_{n>0}^{\text{odd}} \frac{\sin\left(m\pi \frac{x}{a}\right) \cdot \sin\left(n\pi \frac{y}{b}\right)}{mn\left(m^2 k + n^2/k\right)^2} \tag{2}$$

governs the variation of plate deformation as a function of position, being described as a series expansion. Typical elastic constants for glass are $E_{\text{glass}} \approx 70\text{–}75$ GPa and $\mu_{\text{glass}} \approx 0.2\text{–}0.25$.

Equation (1) can be solved for any given set of window dimensions and thus allows to compute the geometrical deformation of a window pane as a function of pressure difference. The position dependence is contained in $\phi(x,y,k)$ i.e. equation (2). This can be easily evaluated e.g. with an Excel spreadsheet program, since the series expansion converges rapidly. For example, using maximum odd numbers of $m = 15$ and $n = 15$, we find for the relative deviation at maximum sag

$$\frac{\phi(m, n \text{ up to } \infty) - \phi(m, n \text{ up to } 15)}{\phi(m, n \text{ up to } \infty)} < 10^{-5}. \tag{3}$$

Once the sag $W(x,y)$ is known, the respective window tilts may be computed from the same program. The absolute value of the tilt is found from

$$t(x, y) = \sqrt{\left(\frac{\partial W}{\partial x}\right)^2 + \left(\frac{\partial W}{\partial y}\right)^2}. \tag{4}$$

For later ray tracing analysis, we use the tilts in the (x-z) and (x-y) directions $\partial W/\partial x$ and $\partial W/\partial y$. The resulting two matrices $\partial W(x,y)/\partial x$ and $\partial W(x,y)/\partial y$ can then be used in a simple ray tracing program to compute the reflected light distribution on a projection screen at a given distance from the window. The quality of the result depends on the number of rays which is defined by the spatial resolution, i.e. the size of the increments dx and dy. In our computations for the square 1 m^2 window we used $200 \times 200 = 40\,000$ area elements. A test with 1000×1000 elements of 1 mm^2 gave essentially the same result, due to the much longer computation time, all other simulations were done with area elements of 5 mm side length. For example we also treated rectangular 2 m^2 windows with $k = 2$, using $400 \times 200 = 80\,000$ area elements of (5 mm)^2 each. In order to reproduce features from the observations we also treated rectangular windows with $k = 1.4$ and 280×200 area elements.

Some details about ray tracing procedures are given in the appendix. We start with light rays having normal incidence with regard to the undisturbed window surface. Due to the tilts $\partial W/\partial x$ and $\partial W/\partial y$ of an area element dx × dy of the deformed window, we can find the angle of incidence and from the law of reflection the direction of the reflected light ray. If a projection screen is in a given distance d from the window ($d \gg W(x,y)$), the position of the reflected light ray due to window position (x,y) is given by:

$$x_{\text{refl}}(x, y) = x - 2d\frac{\partial W(x, y)}{\partial x} \tag{5a}$$

and

$$y_{\text{refl}}(x, y) = y - 2d\frac{\partial W(x, y)}{\partial y}. \tag{5b}$$

All computations are based on the same Excel program having three functions. First it is used to compute $\phi(x,y)$ of equation (2). The program allows to vary the input parameters by setting a prefactor which then results in the sag (equation (1)) and tilt $t(x,y)$ (equation (4)). Once the sag is known, one only needs the distance d of the projection screen from the window as final parameter for solving equation (5).

5.2. Elastic deformations for quadratic and rectangular windows

As expected, maximum sag for rectangular geometry occurs at the center and contours of equal sag are nearly circles for quadratic windows close to the center (or ellipses for rectangular windows), but deform to rounded squares (rounded rectangles) when approaching the perimeter (see figures 12, 13). As a consequence, the tilt is zero at the four corners and at the center, large at the middle of the perimeter and shows a pronounced diagonal symmetry (similar to figures 3, 4 in [11]).

To get a feeling for the magnitude of the sag, we give an example for the center of a quadratic window with $a = b = 1$ m, $h = 5$ mm, $E = 70$ GPa, and $\sigma = 0.20$. The prefactor $\alpha \cdot a^2b^2/h^3$ amounts to $\approx 2.19 \cdot 10^{-5}$ m Pa^{-1}, i.e. 2.19 mm hPa^{-1}. At the center of the window ($x = y = a/2$) the sin functions result in +1 or −1 only and the summation due to the denominator values yields $\phi \approx 0.244$. Therefore the theoretical sag at the center of a 1 m^2 quadratic plate amounts to $W_{\max} \approx \Delta p \cdot 0.53$ mm hPa^{-1}. The respective value for a rectangular window of $\approx$2.2 m^2 ($a = 1.75$ m, $b = 1.25$ m) should give rise to a maximum theoretical sag of

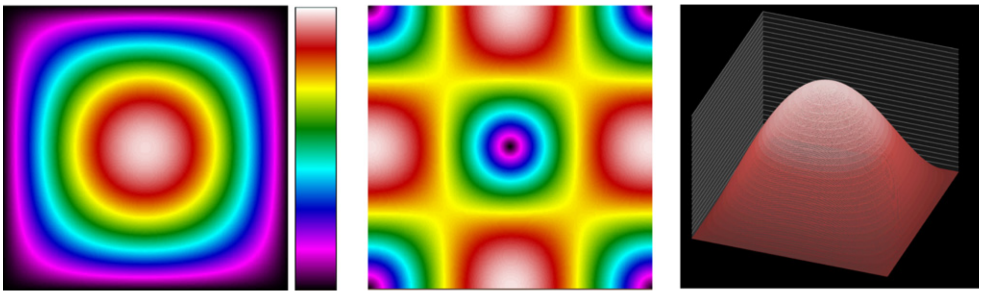

Figure 12. (a) Schematic plot of contours/regions of equal deformation, i.e. sag, of a quadratic 1 m^2 window as computed theoretically (200×200 area elements). These are due to the position dependent factor $\phi(x,y)$ (equation (2)). Close to the center, the shape resembles circles whereas close to the perimeter, the shape is better approximated by rounded squares. (b) Corresponding tilt according to equation (4). The colour bar refers to both (a) and (b). (c) Three-dimensional plot of the sag of figure (a).

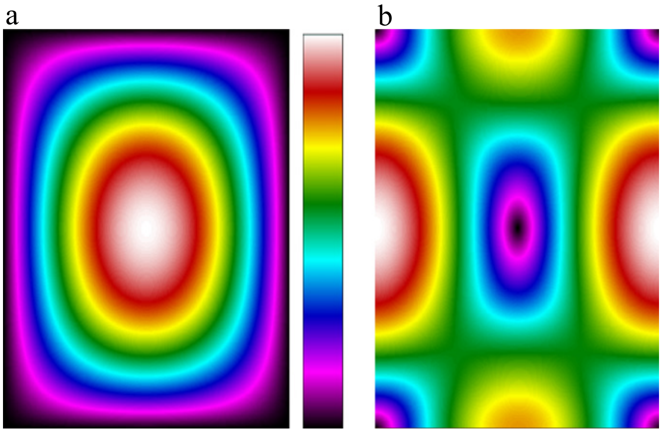

Figure 13. Schematic plot of contours/regions of equal deformation of a rectangular window (a) and respective tilt (b) with aspect ratio $k = 1.4$ (200×280 area elements). Close to the center, the deformations resemble ellipses whereas close to the perimeter, the shape is better approximated by rounded rectangles.

Table 1. Maximum sag for windows of a given area and aspect ratio k for $\Delta p = 1$ hPa.

	$k = 1$	$k = 1.4$	$k = 1.5$	$k = 2$
Area: 1 m^2	0.53 mm	0.48 mm	0.45 mm	0.33 mm
Area: 2 m^2	2.14 mm	1.90 mm	1.81 mm	1.33 mm

around $W_{max} \approx \Delta p \cdot 1.90\,\mathrm{mm\,hPa^{-1}}$. Table 1 gives a summary of the maximum sag for several windows and well defined $\Delta p = 1$ hPa.

The order of magnitude seems reasonable keeping in mind that first, the inner space of double pane windows usually ranges around 15 mm or so and the naked eye cannot detect strong curvatures of such windows. Realistic window values may change depending on material properties. Second, we also manually applied a force of around 100 N (measured with a balance) with a thumb on the center of a 2.2 m^2 window pane of $k = 1.4$ while observing typical changes of the observable caustics similar to those in nature (change from a square-like to a cross-like feature). This point-like stress—if as first approximation interpreted as uniform pressure across the pane—would correspond to about 50 Pa, i.e. 0.5 hPa. For the window area of 2.2 m^2, one would expect a maximum sag of around 1.15 mm for 0.5 hPa. We also measured the manually induced deformation by attaching a solid square rod to the window frame and measuring the distance from the rod to the center of the pane without and with induced pressure. We measured typical maximum maximum sags around 2 mm which is in reasonable agreement with expectations.

5.3. Ray tracing analysis of reflected light distributions: quadratic windows

Next, we discuss the reflection of incident parallel (sun) light from such deformed window panes. For simplicity we start with quadratic windows. If the sag would show spherical symmetry around the axis through the center, the window would represent a concave or convex mirror. Untreated glass surrounded by air has a reflectivity depending on the glass optical constants, e.g. a single pane window of index of refraction $n = 1.5$ typically reflects about 8% of the incident light for normal incidence (due to the two air-glass-boundaries) [10]. For parabolically shaped surfaces, all light would be focused into a single focal point for proper image distance, i.e. the focal length f. For spherically shaped mirror surfaces, only the paraxial rays will be focused into the focal point, light which is incident more distant from the optical axis will form a caustic [6]. Rectangular windows differ from usual mirrors in optics in two aspects: first the surface even of the paraxial rays will neither be spherical nor parabolic.

Second, the diagonal symmetry of the tilts (figures 12, 13) suggests that the focused light should also show this diagonal symmetry as was observed in figures 1 and 5. In addition, what can actually be observed depends on the distance between window and projection wall. If it equals the focal length, one should observe a nice focus, surrounded by some structures with diagonal symmetry. If it is much larger or smaller, the focus is washed out.

Some first exemplary optical simulations [14] by S Wennmacher (a physics teacher student for his final exam work, supervised by H J S, one of the authors) were qualitatively supporting expectations. Here more quantitative simulations using Excel spread sheets will be discussed.

Figure 14 shows some typical results as point scatter plots for reflected light for a well defined distance $d = 50$ m of the projection screen for a quadratic window (1 m^2) acting as concave mirror and a maximum sag of 1 mm. The optical reflections are due to two different contributions from the concavely shaped pane (light focusing) and the convexly shaped pane (defocussing). Since the panes are only a few mm thick, deformations are small and we are dealing with normal incidence light, we only consider the effect of a single reflection from each pane, i.e. we assume that the second reflection from the back side of each pane more or less coincides with those from the front sides and just changes the amount of radiation but not the light distribution on the projection screen.

Figures 14(a) and (c) separately depict the contributions from the concavely and convexly formed panes. For size comparison, the broken line square gives the dimensions of the reflecting window. The different scale is due to different effects of focusing and defocussing. These shape plots of the light distribution define the contours which are observed with the naked eye. Figure 14(b) shows an irradiance plot for figure 14(a), which nicely shows the strong enhancement within the focal area which could be measured with a power meter.

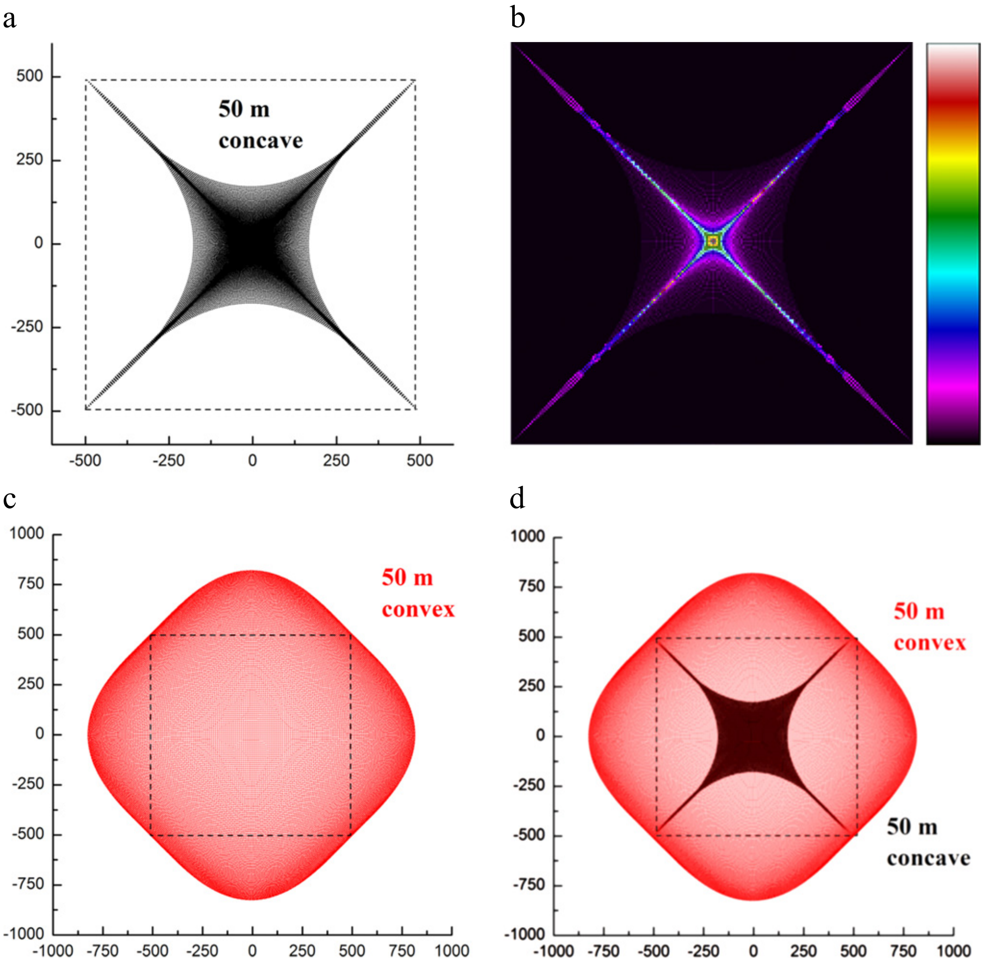

Figure 14. Overview of caustic features upon normal incidence due to a 1 m^2 quadratic window (200×200 area elements) with maximum deformation of 1 mm (corresponding to $\Delta p \approx 1.9$ hPa) in a distance of 50 m. (a) Shape due to concavely formed pane; (b) irradiance plot of the data for (a) with false colour scale; (c) shape due to convexly formed pane; (d) superposition of concave and convex contributions, corresponding to observations. Note the change of scale which is −500 mm to 500 mm each side in (a) and (b) and −1000 mm to 1000 mm each side in (c) and (d). The broken line square shows the size of the original window panes for size comparison.

Most of the following plots will be of the type shown in figure 14(d), which are overlay plots of both panes. In this case, for the quadratic window, one sees that both light contributions have diagonal symmetry as expected.

Figure 15 shows a comparison for light distribution plots as a function of distance for the same quadratic window. One can see that for distances around 50 to 70 m a region with large irradiance (focal area) evolves. In the present case a distance of around 62.5 m was giving more or less the highest irradiances. The outer shape resembles a square for large distances which turns into a rounded square or circle for small distances. These plots also qualitatively explain what happens if the maximum deformation changes. An increase in maximum

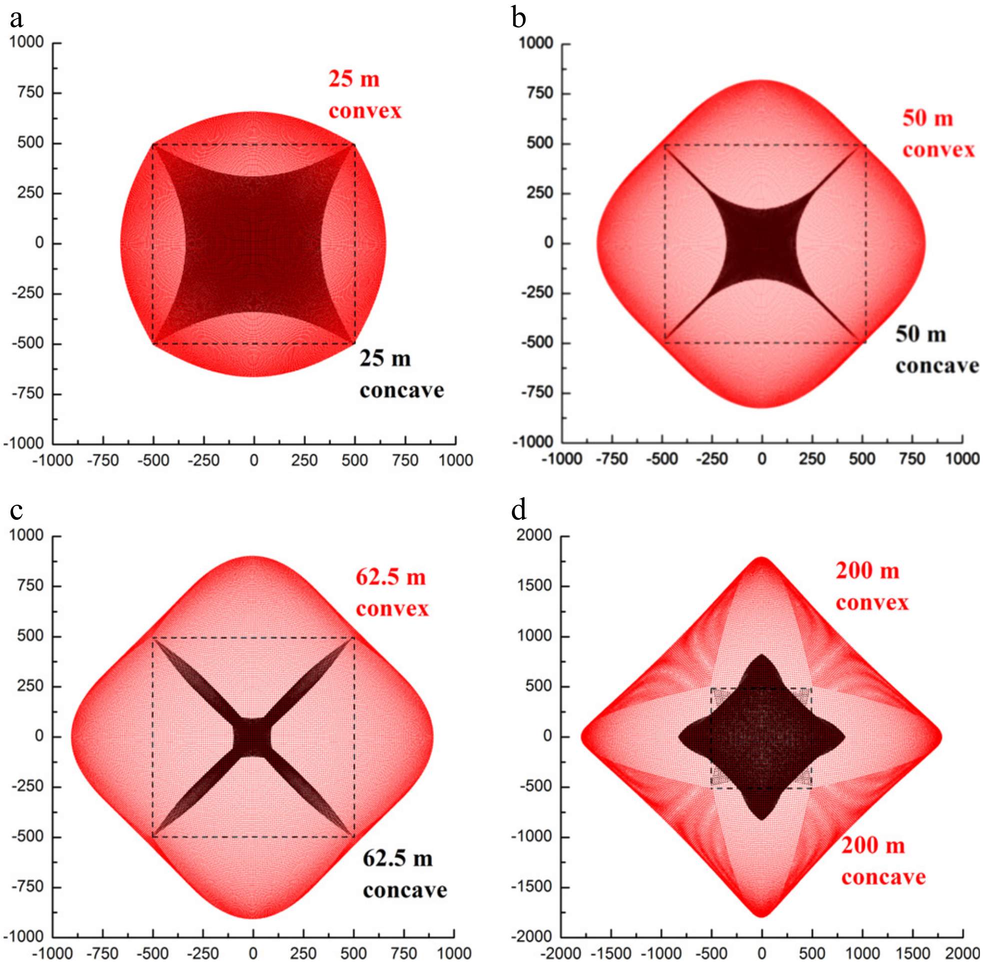

Figure 15. Light distribution plots from a 1 m^2 quadratic window on a projection screen in distances from 25 m via 50 m and 62.5 m to 200 m (normal incidence, maximum deformation 1 mm). Please note the scale change for 200 m.

deformation directly translates into an increase in the value of the partial derivatives which define the reflected light spot. Therefore, an increase of maximum sag has the same effect as an increase of distance.

In order to better understand the physics behind these images, i.e. which regions on the window panes are responsible for specific features within the caustic, figure 16 shows some contour lines due to reflected light from area elements along vertical lines of the deformed window. Figure 16(c) depicts the position of the chosen vertical line elements on the deformed windows. Figure 16(a) shows results side by side with half of the full projection image (figures 14(a), (c)) for a concavely deformed, i.e. focusing window pane, figure 16(b) depicts the same for a convexly, i.e. defocusing pane.

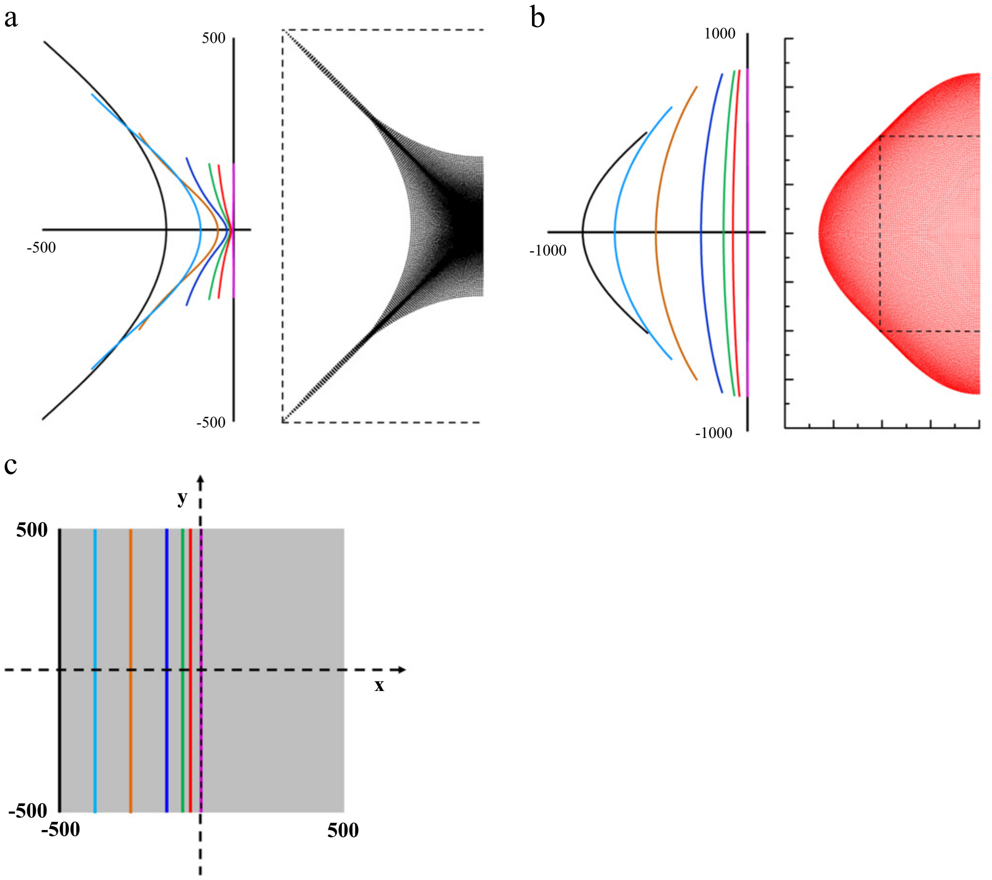

Figure 16. (a), (b) Plots of the position of reflected light due to vertical lines at the surface of a quadratic 1 m^2 window with maximum sag of 1 mm at a projection distance 50 m for a concavely (a) and convexly (b) deformed pane. The quadratic window extended from −500 mm to +500 mm. The seven arbitrarily chosen lines (c) from left to right: −500 mm; −375 mm; −250 mm; −125 mm; −65 mm; −40 mm; 0 mm (center line).

5.4. Ray tracing analysis of reflected light distributions: rectangular windows

Many windows in buildings are rectangular with aspect ratios varying around 1.4 and 1.5. Since the windows responsible for the observations shown in figures 2 and 5–8 were due to $k = 1.4$, we present respective theoretical simulation results.

Figure 17 depicts results for a window of 2.18 m^2 (1.25 m × 1.74 m) for 0.9 mm sag, corresponding to a pressure difference of around 0.4 hPa. In general, the reflected light distributions have similar features than those of the quadratic window, the main difference being that the focal features are stretched along the vertical direction. The concave, focusing pane gives rise to an extended cross-like structure whereas the convex defocusing pane yields the outer rhombic-like feature.

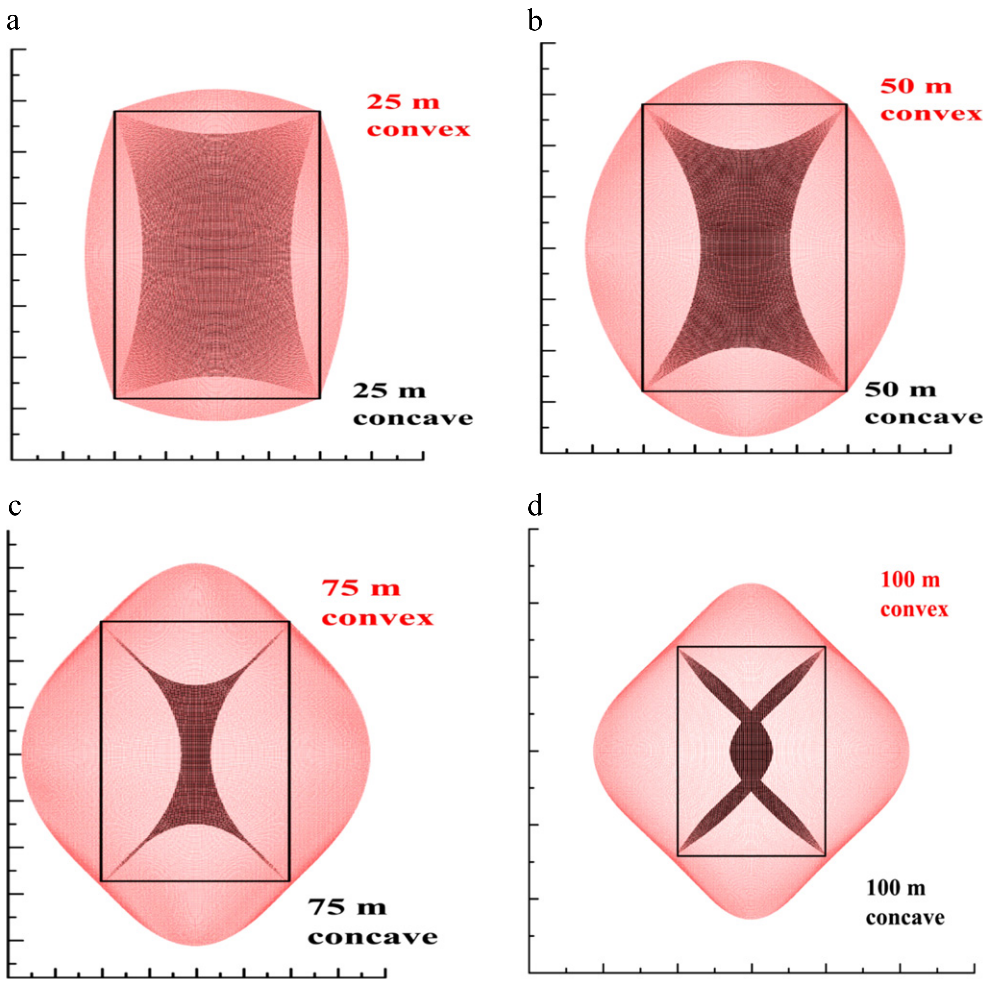

Figure 17. Overview of superimposed reflected light distributions from convex as well as concave panes upon normal incidence due to a rectangular window ($k = 1.4$, 200×280 area elements) with maximum deformation of around 0.9 mm (corresponding to $\Delta p \approx 0.4$ hPa) as a function of distance of a projection screen. Distances vary from 25 m via 50 m and 75 m to 100 m. Note the change of scale which is −1000 mm to 1000 mm each side in (a) and (b), −1200 to 1200 in (c) and −2000 mm to 2000 mm each side in (d). The black rectangle shows the size of the original window panes for size comparison.

5.5. Comparison to observations

Figure 18 shows some examples of observed features which were qualitatively modeled (inserts) with appropriate parameters for pressure difference, elastic constants and dimensions of the windows (after [7]). In principle, each concavely or convexly shaped pane would lead to reflection from both the front and the back interface. However, since near normal incidence was studied, the second reflection would only lead to a very small smearing out of the features. Therefore, for simplicity only a single reflection from each pane was treated.

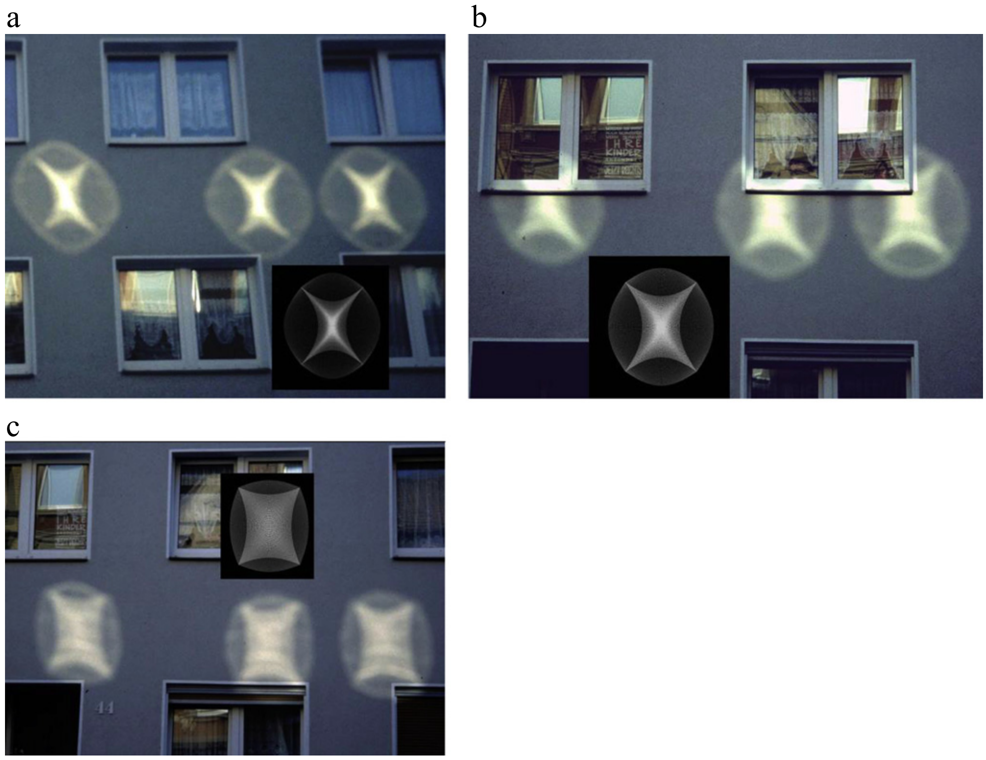

Figure 18. Examples of optical features upon reflection from the same curved window panes, observed at different days with changing atmospheric pressure (after [7]). The windows had a height versus width ratio of 3:2, i.e. $k = 1.5$. In (a) the pressure difference was largest, in (b) intermediate and in (c) lowest. The inserts show results of exemplary theoretical simulations, while varying the pressure difference. Even in (a) the condition with distance close to the focal distance was not yet reached.

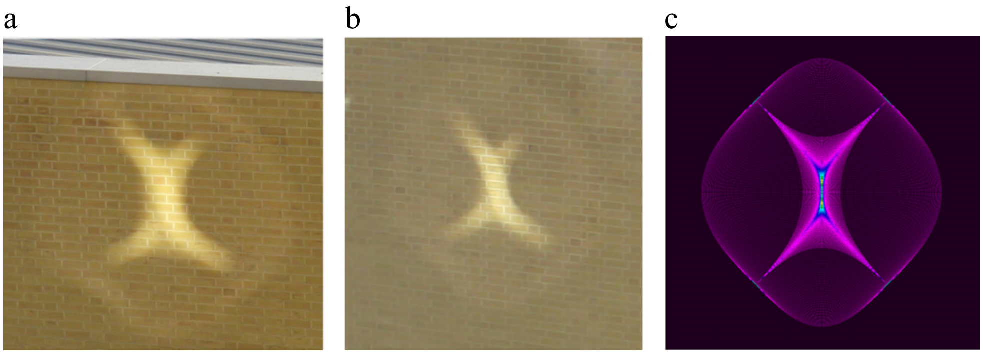

Figure 19. Comparison of two observed reflection features (a), (b) of a rectangular window (height versus width ratio $k \approx 1.4$) with a simulation result (c). The inner cross-like feature as well as the outer rhombic feature are clearly reproduced.

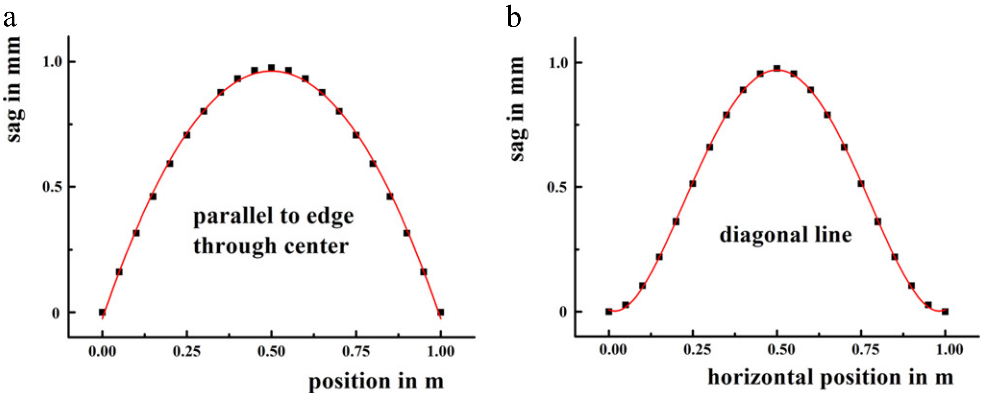

Figure 20. Sag along vertical (a) and diagonal line (b) passing through the center of a quadratic window (compare figure 12) with 1 mm maximum sag. The plotted straight lines resemble polynomial fits of 2nd order for the vertical and 4th order for the diagonal line.

The comparison in figure 18 is qualitative only. Quantitative comparison was not done since the actual pressure difference was not known. In principle the pressure difference could be estimated if it would be easily possible to vary the projection distance (which is not the case) such that the focal distance could be estimated and therefrom the expected theoretical pressure difference (see section 6).

Figure 19 depicts a comparison between two observed features from a rectangular window with k = 1.4 (figures 19(a), (b)) with the quantitative theoretical approach from above (figure 19(c)). Figure 19(c) corresponds to figure 17(c) but represents the respective expected irradiance distribution. The inner cross-like feature as well as the outer rhombic feature have the highest irradiance and their geometric forms nicely correlate to observations, also regarding the fact, that the outer rhombus has maximum strength at the center of the lines and is lowest for the four corners.

Typical measurement distances of observations were around 30 to 40 m and quite good agreement can be found. From equations (1) and (5) it is obvious, that each result in figure 17 holds for a number determined by the product of pressure difference and distance. This means that, e.g., the result for $d = 75$ m and $\Delta p = 0.4$ hPa equals the one for $d = 37.5$ m and $\Delta p = 0.8$ hPa. From a comparison between observation and simulations, we expect that for the simulation conditions, with $\Delta p = 0.4$ hPa, distances between, say, 60 to 80 m are in good agreement. Therefore we expect typical pressure differences of the order of 0.5 to 1 hPa to cause the phenomenon. Before discussing whether such numbers are reasonable from meteorological changes, we first briefly discuss of how to find focal distances from the model.

5.6. Estimating focal lengths from window curvatures: presence of astigmatism

Once the curvature of the window pane is known theoretically, one may easily estimate focal lengths. This can be done first by using the ray tracing program and searching for maximum irradiance in plots like figure 15. Second, a rough estimate may use an average tilt angle and apply the law of reflection. Third, as will be done below, one may use second order fit functions, i.e. parabolas, to approximate theoretical deformations.

For rectangular or quadratic windows with given maximum sag, the tilts for various directions differ. Therefore, the sag as function of position along various lines along the window differ and one should also expect a change of the respective focal distances. As an example figure 20 depicts vertical and diagonal line plots through the center for the sag of quadratic windows (some points marked) together with polynomial fits (solid lines).

The vertical line shows maximum tilt at the edge and can be very accurately fitted with a parabola. In contrast, the diagonal line—due to the model assumptions—has fixed zero sag at the corners. Therefore the best fit is a 4th order polynomial. However, assuming that most prominent features of the reflected light are due to regions with large tilt, it makes sense to also fit just the central part. This may also be approximated by a second order polynomial.

As an example for the order of magnitude of theoretical focal distances, we used the equation for the vertical line parabola for a maximum sag of 1 mm for a quadratic window. Its parabolic line fit (figure 20(a)) is approximately given by

$$y = \frac{4}{1000} \cdot \left(-x^2 + x \right) \tag{6a}$$

where y is the sag in m and x the position along the window in m. Obviously the number 4 from the fit is directly proportional to the sag. Transforming this parabola into its normal form

$$y = \frac{4}{1000} \cdot x^2 \tag{6b}$$

and knowing from mathematics that a parabola normal form can be written as

$$y = \frac{1}{2p} \cdot x^2 \text{ with } f = \frac{p}{2} \tag{6c}$$

we find $4/1000\ \mathrm{m}^{-1} = 1/(2p)$, i.e. $p = 125$ m and we can immediately locate the focal point F in the focal distance $f \approx 62{,}5$ m. Such a distance is very reasonable for actual observations.

Fitting the center part of the diagonal line for the quadratic window, we do however, find a focal length which (depending on the chosen center section for the fit) can be up to a factor 1.7 smaller, i.e. we would find focal lengths of only 37 m or so. This argument easily explains why window reflections should always have some astigmatism, i.e. there will never be a single perfect focus but always regions around some critical focal distance with a concentration of light in small areas, leading to large irradiances.

Finally, equation (6*c*) also explains how focal distance changes with sag. A larger sag value (a number larger than the 4 from above) will decrease p and according to equation (6*c*) the focal length f.

6. Window deformations due to ambient pressure and temperature changes

The lab experiment of section 4 demonstrated the optical effect and allowed measurements of pressure differences related to pane deformations. We now apply the theory for the pane deformation from section 5 to the experimental model window. We used an acryl glass model with $a = b = 0.185$ m, $h = 3.5$ mm and inner gap of 5 mm. According to tables for acryl glass, Young's modulus is around 3.0 to 3.3 GPa. Whatever value is chosen this is much lower than the one for glass. Also the Poisson ratio is slightly higher, e.g. $\mu_{\mathrm{acryl}} \approx 0.35$. For $E_{\mathrm{acryl}} = 3.2$ GPa, the maximum sag should be around 0.037 mm hPa^{-1}, giving around 0.9 mm for $\Delta p = 25$ hPa. This is already of the same order as the experimentally observed value of 0.5 mm (figure 11). The difference is partly due to uncertainties in the parameters for acryl glass, the main effect is, however, probably due to the chosen boundary condition of the theory. Equations (1), (2) were derived for the assumption that the pane is fixed at the boundary lines of the rectangular perimeter. Therefore, although there were no deformations

Table 2. Function Θ (k) and prefactor C of swept out volume of a single pane for windows of a given area and aspect ratio k.

	$k = 1$	$k = 1.4$	$k = 1.5$	$k = 2$
Θ (k)	0.1023	0.0917	0.0874	0.0662
ΔV (1 m^2)	2.24×10^{-6} m^3 Pa^{-1}	2.00×10^{-6} m^3 Pa^{-1}	1.91×10^{-6} m^3 Pa^{-1}	1.45×10^{-6} m^3 Pa^{-1}
ΔV (2 m^2)	1.79×10^{-5} m^3 Pa^{-1}	1.61×10^{-5} m^3 Pa^{-1}	1.53×10^{-5} m^3 Pa^{-1}	1.16×10^{-5} m^3 Pa^{-1}

at the perimeter, tilts were possible. In reality, the windows are attached to the window frame in a rather stiff way. This decreases the perimeter tilts and therefore also change the theoretical deformations all across the window. A respective analysis is way beyond the scope of this article.

Nevertheless, the model experiments of section 4 showed very close agreement of the caustic features due to real windows. However, clever students may detect a difference to the daily life observations, i.e. that the situation differs appreciably from real double pane windows. In the (isothermal) experiment, pressure within the panes was changed with regard to the outside atmospheric pressure by changing the number of gas molecules in the inner volume using a syringe or the vacuum or pressure pump and the measured inner pressure was directly giving the pressure difference between inside and outside. In contrast, for real windows, the inner volume is air tight, i.e. the inside amount of air molecules is fixed and deformations are due to changes of ambient pressure and/or temperature with regard to conditions during the manufacturing.

6.1. Inner gas treated as ideal gas upon pressure and temperature changes

We first assume that filling with gas and sealing of the window was taking place at initial pressure p_0 and temperature T_0. As a consequence, if ambient pressure and temperature are equal to p_0 and T_0, the panes are not deformed and the inner cuboid shaped volume V_0 is defined by the window area A and the inner pane separation d (e.g. left scheme of figure 3). If external conditions change, the window panes are deformed either inward (e.g. right scheme of figure 3) or outward. We assume that external pressure is given by $p_{ext} = p_0 + \Delta p_{amb}$ and temperature $T = T_0 + \Delta T_{amb}$. As a consequence, the window deforms. Due to the elastic constant of glass it deforms until an equilibrium is established with a pressure difference Δp between inside and outside which usually differs appreciably from Δp_{amb} (see below).

For given pressure difference Δp, the inner volume change ΔV between the two panes is calculated by integrating the sag across the window area A, which gives [11]:

$$\Delta V = 2C(k) \cdot \Delta p \tag{7}$$

with

$$C(k) = \frac{192(1 - \sigma^2)}{\pi^6 E} \cdot \frac{A^3}{h^3} \cdot \Theta(k) \tag{8}$$

Θ (k) is a function [11] which only depends on the aspect ratio of the window. Table 2 gives respective values as well as values for $C(k)$, again for windows with areas of 1 m^2 and 2 m^2, $h = 5$ mm, $E = 70$ GPa and $\sigma = 0.20$.

For example, a pressure difference of 1 hPa would result in a swept out volume of a single quadratic 1 m^2 window pane $C\Delta p = 2.24 \times 10^{-4}$ m^3.

For the following example, we assume initial conditions as follows: $p_0 = 1000\,\text{hPa}$, $T_0 = 300\,\text{K}$, and $V_0 = 15 \times 10^{-3}\,\text{m}^3$ (for an inner spacing of 15 mm). Assuming the ideal gas law, we find upon external changes Δp_{amb} and ΔT_{amb} while keeping N constant, and assuming that the glass panes and inner gas will have ambient temperature.

$$\frac{p_0 \cdot V_0}{T_0} = \frac{\left(p_0 + \Delta p_{\text{amb}} + \Delta p\right) \cdot \left(V_0 + \Delta V\right)}{T_0 + \Delta T_{\text{gas}}}. \tag{9}$$

Here, the inner pressure is written as external pressure $p_{\text{ext}} = p_0 + \Delta p_{\text{amb}}$ plus the actual pressure difference Δp between inside and outside. $\Delta T_{\text{gas}} = \Delta T_{\text{gas}}(\Delta T_{\text{amb}})$ describes how the inner gas temperature depends on the ambient temperature difference ΔT_{amb}. This will be discussed below. Inserting equation (7) into equation (9) and solving for Δp we find:

$$\Delta p = \frac{\left(p_0 \cdot \Delta T_{\text{gas}} - \Delta p_{\text{amb}} \cdot T_0\right) \cdot V_0}{T_0 \cdot \left[2C(k) \cdot \left(p_0 + \Delta p_{\text{amb}} + \Delta p\right) + V_0\right]}. \tag{10}$$

We can safely assume that Δp in the denominator is smaller than Δp_{amb} and both are much smaller than p_0. Since $2C(k)\, p_0$ is at least an order of magnitude larger than V_0 (e.g. $2Cp_0 = 0.45\,\text{m}^3 \approx 30 \cdot V_0$ for a 1 m^2 square window) we have:

$$\Delta p \approx \frac{\left(p_0 \cdot \Delta T_{\text{gas}} - \Delta p_{\text{amb}} \cdot T_0\right) \cdot V_0}{T_0 \cdot 2C(k) \cdot p_0}. \tag{11}$$

6.2. Solutions for isothermal, isobaric and general case

6.2.1. Isobaric. Pressure and temperature changes may be treated separately first, before discussing their combined action.

For isobaric conditions, i.e. $\Delta p_{\text{amb}} = 0$, equation (11) can be simplified to give

$$\Delta p \approx \frac{\Delta T_{\text{gas}}}{T_0} \cdot \frac{V_0}{2C}. \tag{12}$$

The temperature difference ΔT_{gas} refers to the one of the gas in the sealed inner spacing between the panes. This is related to a temperature difference ΔT_{amb} between inside and outside of the building which is usually easy to measure. Let us assume that the typical inside temperature $T_{\text{in}} = 20\,°\text{C}$ is the temperature at which the inner gas volume was sealed. A very dramatic T change would occur in winter for outside temperatures below freezing, e.g. for $T_{\text{out}} = -10\,°\text{C}$, i.e. $\Delta T_{\text{amb}} = 30\,\text{K}$. The temperature change within the window of a double pane window for this temperature gradient was calculated, assuming glass thickness of 4 mm with thermal conductivity of $1\,\text{W}(\text{m} \cdot \text{K})^{-1}$, inner air spacing of 10 mm with thermal conductivity of $0.026\,\text{W}(\text{m} \cdot \text{K})^{-1}$, and standard heat transfer coefficients of $\alpha_{\text{in}} = 8\,\text{W m}^{-2}\text{K}^{-1}$ for the inside and $\alpha_{\text{out}} = 25\,\text{W m}^{-2}\text{K}^{-1}$ for the outside surface (section 4.3.4 in [15]). In this case the two glass surfaces, which are the boundaries of the inner gas, had temperatures of 13.3 °C and 13.1 °C respectively, which resembles a ΔT_{gas} of only around 7 K. The fact that ΔT_{gas} is much smaller than ΔT_{amb} was of course expected since thermal insulation was the main motivation for using such windows. It is probably safe to assume, that if ΔT_{amb} is given, the respective ΔT_{gas} is at most one quarter of it. Using $\Delta T_{\text{amb}} = 30\,\text{K}$, i.e. $\Delta T_{\text{gas}} = 7\,\text{K}$ and $V_0/(2C) \approx 67\,\text{hPa}$ (1 m^2 quadratic window), we find $\Delta p \approx 1.6\,\text{hPa}$ (similarly the value is around 0.22 hPa for a 2 m^2 rectangular window with $k = 1.4$). Since ΔT_{gas} will have the same sign as ΔT_{amb}, the shape of the inner gas volume will be convex for $\Delta T_{\text{amb}} > 0$ and concave for $\Delta T_{\text{amb}} < 0$.

These pressure differences of the order of 1 hPa are in agreement with expectations from above.

6.2.2. Isothermal. Next we assume isothermal conditions between inside and outside, i.e. $\Delta T_{\mathrm{amb}} = 0$ which also means $\Delta T_{\mathrm{gas}} = 0$. Similar to the arguments from above, equation (11) can now be simplified to give

$$\Delta p \approx -\frac{V_0}{2C} \cdot \frac{\Delta p_{\mathrm{amb}}}{p_0}. \tag{13}$$

Using $\Delta p_{\mathrm{amb}} = 20$ hPa, and $V_0/(2C) \approx 67$ hPa (1 m^2 quadratic window), we find $\Delta p \approx -1.34$ hPa (or similarly 0.19 hPa for rectangular 2 m^2 window with $k = 1.4$). Obviously though maybe unexpected at first naïve glance at the problem, the change of internal gas pressure is more than a magnitude smaller than the ambient pressure difference. The minus sign is related to the shape of the inner gas volume: it will be concave for $\Delta p_{\mathrm{amb}} > 0$ (i.e. $\Delta p < 0$, internal pressure smaller than ambient pressure) and convex for $\Delta p_{\mathrm{amb}} < 0$ (i.e. $\Delta p > 0$, internal pressure larger than ambient pressure).

The physics reason for the actual pressure difference being much smaller than the ambient pressure change is simple. If an ambient pressure change of e.g. +30 hPa would transfer into an actual pressure change of the same magnitude (e.g. more than 10 hPa), the deformations (table 1) would be comparable to the inner spacing. As a consequence, the induced volume change would be comparable to the total inner volume. Treating such an induced volume change as isothermal, the resulting inner pressure change would be very large, probably larger than the induced external pressure which contradicts the argument. Obviously, the interplay between external pressure and therefrom induced inner pressure rise automatically leads to a much lower actual pressure difference.

6.2.3. General case. Comparing results from equations (12) and (13), we also see that for reasonable changes of ambient temperature and pressure, the respective changes of internal gas pressures are of the same order of magnitude.

Allowing both temperature and pressure to change simultaneously from the predefined manufacturing values, we now discuss equation (11) for sun shine conditions, which are needed to observe the optical phenomena due to the deformations. Typical weather conditions with sun shine in Western European summertime are high pressure and high temperatures ($\Delta p_{\mathrm{amb}} > 0$ and $T_{\mathrm{amb}} > 0$). In wintertime, sunny and cold periods are usually also characterized by high pressure systems ($\Delta T_{\mathrm{amb}} < 0$ and $\Delta p_{\mathrm{amb}} > 0$), usually with even higher pressure than in summer, due to the much colder air. In contrast, mild winters are usually associated with low pressure systems and rainy weather which does not allow observations of the phenomenon. In spring and fall, conditions can vary. For the dates of our observations, e.g. the 25th of November 2011 a high pressure system resulted in more than 1030 hPa at our location and outside temperatures when photos were recorded were around 5 °C.

If both temperature and pressure differences will have the same sign, their effects are counteracting and the overall pressure difference can be small. However, whenever high pressure is associated with low temperature or vice versa, both effects add up and the overall deformation will be large.

Using equation (11) with appropriately analyzed $\Delta T_{\mathrm{gas}}(\Delta T_{\mathrm{amb}})$ will give the pressure differences which are responsible for the deformation. Our observations (figures 2, 5–7) were from 25th of November 2011 for temperatures between 3 °C and 5 °C and very high pressure above 1030 hPa. The respective pressure changes Δp due to temperature and ambient pressure

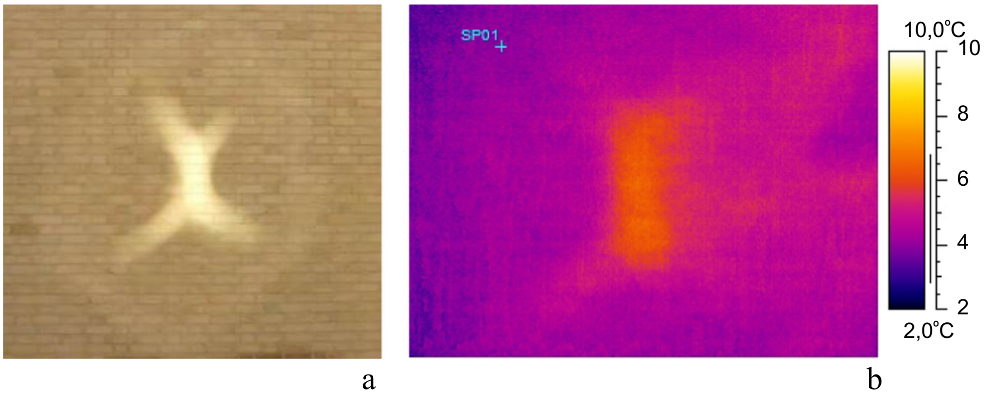

Figure 21. Enlarged section of light focus due to reflected sunlight from a double pane window on the wall of a neighbour building (a) and respective surface temperature distribution (b). The temperature increased by about 2 K due to the irradiance, the spot moving from right to left due to the changing position of the Sun.

changes add up to yield around $\Delta p_{\mathrm{tot}} \approx 2.9$ hPa (1 m^2 quadratic window) or 0.4 hPa (2 m^2 window with $k = 1.4$).

These values are very realistic and would give rise to maximum sags of the order of 1 mm for windows (table 1).

So far, we have assumed a certain manufacturing pressure of, say, 1000 hPa. Now one can easily imagine that the window manufacturing occurs at a certain elevation above sea level, but the windows are sold all over the country, i.e. also at locations with different elevation. A quick survey of window manufacturers in Germany revealed quite a few businesses producing at heights well between near sea level to about 500 m. If sold to regions with different heights, the height difference can give rise to pressure difference offsets, i.e. respective windows may show deformations all the time.

Assuming that production would take place at sea level with average pressure of 1000 hPa, one can estimate the pressure change with height change h for an isothermal atmosphere from the barometric formula

$$p(h) = p(0) \exp\left\{ -h/H \right\} \tag{14}$$

where H is the scaling height of about 8000 m.

Some typical values for such height related pressure differences $\Delta p_{\mathrm{height}}$ are $\Delta p_{100\mathrm{m}} = 12.4$ hPa, $\Delta p_{200\mathrm{m}} = 24.7$ hPa, $\Delta p_{300\mathrm{m}} = 36.8$ hPa, or $\Delta p_{500\mathrm{m}} = 60.6$ hPa. These values are comparable to naturally occurring pressure differences due to normal weather changes of about +−30 hPa with regard to average pressure.

Finally, we mention that the fact that windows do indeed show the observed optical effects even after years is an indication that the inner gas volume is indeed quite well sealed.

7. Thermal effects due to the reflected light distributions

A few years ago, there were many news reports (e.g. [9]) dealing with sunlight reflections of a Las Vegas skyscraper with very pronounced thermal effects [6]. The respective irradiances were much higher than from an individual window (many windows contributed simultaneously) nevertheless the news reports also mentioned thermal effects due to individual windows. In particular it was argued that the decorative vinyl outer coating of some houses in the US was damaged by focused light from double pane windows of nearby houses. In order to test this hypothesis we measured the irradiance within focal areas of the reflection caustics and also studied associated thermal effects on the wall of a neighbour building.

The caustics with the form of brightly illuminated focal areas with the geometry of the letter *X* as those observed in figures 1 and 5–7 consist of focused light, i.e. the irradiance at the wall surface is larger than the one at adjacent wall sections. Therefore, thermal effects are to be expected. Figure 21(a) depicts an enlarged version of such a caustic feature observed from close distance. The window causing this feature was in a distance of about 30 m having a size of $1.25 \times 1.74\ \mathrm{m}^2$. On the wall, the width of the focal area corresponded to around 24 cm (about the width of a single brick) with a vertical extension of about 65 cm (height of about eight bricks).

Whenever light from a large area is focused to a much smaller area, the irradiance increases with regard to the adjacent wall regions, which lie in shadow and are only illuminated by diffusely scattered sunlight. As a result the focal area equilibrium temperature will increase. The effect due to a single window focusing sunlight via reflection was analyzed with infrared thermal imaging [15, 16]. A LW IR camera, operating in the wavelength range from 8 to 14 μm, pointed at the wall area. The result is shown in figure 21(b). The temperature increase at the center of the focal area amounted to about 2 K with regard to the shadow regions of the wall. The situation changes quite rapidly: the reflection was at a distance of about 30 m from the window. Within one minute the Sun moved by about (1/4)° leading to a change of (1/2)° of the reflected beam. This corresponds to a distance of about 25 cm on the wall, covered within one minute. Therefore, transient effects of heat conduction tend to decrease the temperature increase.

Obviously, the maximum observable temperature rises and the respective time constants and transient behavior depend on the irradiance which is available, the ability to absorb sun radiation of the wall, the heat capacity and heat conductivity of the wall as well as its ability to loose energy via conduction, convection and radiation [15].

A very rough estimate can help to understand the effect. The $2.2\ \mathrm{m}^2$ window has about 4% reflectivity from each surface. Two surfaces from a pane contribute to the focusing (the remaining two for defocusing), which means that for a sunny day of, say, $1000\ \mathrm{W\ m^{-2}}$ and normal incidence at sea level, about 8% will be reflected towards the focus. The sun elevation was about 40° which reduces the incident power for vertically oriented windows to about 77%, giving a total of the reflected radiation of $0.08 \cdot 0.77 \cdot 1000\ \mathrm{W\ m^{-2}} \cdot 2.2\ \mathrm{m}^2 \approx 135\ \mathrm{W}$. This radiation is illuminating the focal area of about $0.25 \cdot 0.65\ \mathrm{m}^2 = 0.16\ \mathrm{m}^2$. Taking into account the areas of adjacent optical features around the *X*, we assume an area of, say $0.3\ \mathrm{m}^2$ to which the radiation is focused. This leads to an irradiance of $135\ \mathrm{W}/0.3\ \mathrm{m}^2 \approx 450\ \mathrm{W\ m^{-2}}$ which—as expected from the only 2 K temperature rise—is still much less than if the wall would be in full sunlight.

The argument was checked by measuring irradiances at a sunny and clear blue sky day. The direct irradiance was about $1000\ \mathrm{W\ m^{-2}}$, the diffuse irradiance in the shadow region outside of the reflected light focus was $\approx 150\ \mathrm{W\ m^{-2}}$ and the maximum irradiance in the focus was up to $650\ \mathrm{W\ m^{-2}}$. Neglecting the diffusely scattered light contribution, the increase of irradiance within the focus of about $500\ \mathrm{W\ m^{-2}}$ is in agreement with the estimate of $450\ \mathrm{W\ m^{-2}}$. For one window with very good focus, i.e. small focal area, we could even reach $900\ \mathrm{W\ m^{-2}}$, i.e. almost the direct sun irradiance!

The amount of temperature rise due to this irradiance then depends on the properties of the object which is irradiated. One may expect that thick solid state materials such as the bricks of the wall will only warm up slowly due to their large heat capacity. For an irradiance of $500\,\mathrm{W\,m^{-2}}$, we would expect 80 W within the focal area $A = 0.16\,\mathrm{m}^2$. Due to the Sun movement, each part of the surface is irradiated for about 1 min, i.e. 60 s, giving an available energy for absorption of 4800 J. Accounting for scattering losses we assume that a maximum of about 4000 J will be absorbed. Bricks—being stones—usually have a thermal conductivity which is at least a factor of 10 higher than the one from dry wood. Assuming a thickness of 5 mm we estimate a heated volume of around $8 \times 10^{-4}\,\mathrm{m}^3$ and a mass to be heated of about 1.6 kg. Together with a specific heat of around $1\,\mathrm{kJ\,(kg\,K)^{-1}}$, a temperature rise of about 2.5 K is to be expected. Considering all assumptions in this estimate, the rough agreement with the observed 2 K is satisfactory.

Thinner objects with poor thermal contact to the underlying wall would, however, experience a much faster as well as stronger heating. This argument is also supported by experiments where thin sheets of black paper or plastic foil were in the (well defined) sunlight focus of a cylindrical mirror of around $0.2\,\mathrm{m}^2$ area and were heating up well above 100 °C within a few seconds. Even 1.5 cm thick wooden boards heated up above 100 °C within several minutes [6]. Hence, thin plastic sheets on top of a wall within the focal areas of reflection from double pane windows could heat up better. Therefore, damage on vinyl coatings of houses due to the caustics of double pane windows from neighbour buildings [9] may in principle be possible. However, this would need normal irradiances above $1000\,\mathrm{W\,m^{-2}}$ since otherwise the irradiance of the unobscured sun could already cause a damage. Such high irradiances may be possible for architectural glass with higher reflectivities than the one of uncoated glass panes.

8. Conclusions

Double pane windows show interesting every day optical phenomena in reflected sunlight. They are due to elastic deformations of the panes which lead to concave or convex mirror-like shapes whenever a pressure difference exists between inside pressure which was defined during the production process of the air tight window and outside ambient pressure. Sometimes such windows can very effectively focus light if the distance to a projection screen such as a neighbouring house wall equals the focal distance of the curved mirror-like window. The increased irradiance in focal areas leads to thermal effects which can be detected using infrared thermal imaging. The pressure differences between inside and outside, which are responsible for the deformations can be guessed from an ideal gas model and all optical features can be understood using a simple ray tracing approach. For classroom use, the effect may in addition be demonstrated with miniature model windows.

Appendix: Light reflection at normal incidence from arbitrarily deformed windows

We use the most straightforward approach to follow reflected light rays with vector geometry. Once the sag $W(x,y)$ of the window is known (or computed from equation (1)), all other computations can be done with a spreadsheet program such as Excel. The calculation holds for normal incidence onto the undisturbed window. The extension for arbitrary incidence is possible.

(a) Characterization of surface and light rays

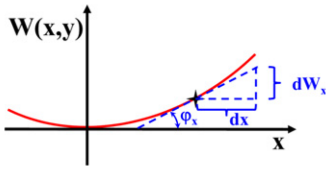

Figure A1. Section of the (xz)-plane, illustrating the partial derivative of sag $W(x,y)$ versus distance along the x axis.

Assuming the incident light to propagate along the z-axis and the undisturbed window to be in the xy-plane, the starting point is the deformation function, i.e. a sag $W(x,y)$ of the reflecting surface. The total window area of size L_x and L_y is approximated by small area elements dx*dy with $L_x = N_x$*dx and $L_y = N_y$*dx. For example, for $L_x = L_y = 1$ m we used $N_x = N_y = 200$, giving 40 000 area elements of (5 mm)^2.

(b) Calculating the orientation of area elements

The sag $W(x,y)$ is used to compute the slope of the area elements in x and y direction (figure A1):

$$\tan\phi_x = \frac{\partial W(x, y)}{\partial x} = W_x' \text{ and } \tan\phi_y = \frac{\partial W(x, y)}{\partial y} = W_y'. \tag{A1}$$

The respective tangent vectors at $W(x,y)$ along the (x,z) direction $\vec{a}_{x,z} = \begin{pmatrix} dx \\ 0 \\ dW_x \end{pmatrix}$ and $\vec{b}_{y,z} = \begin{pmatrix} 0 \\ dy \\ dW_y \end{pmatrix}$ along the (y,z) direction define the area element of the deformed window section. The unit vector $\vec{n}$ orthogonal to the area element is defined by $\vec{n} \propto \vec{a}_{x,z} \times \vec{b}_{y,z}$

$$\vec{n} = \frac{1}{\sqrt{W_x'^2 + W_y'^2 + 1}} \begin{pmatrix} -W_x' \\ -W_y' \\ 1 \end{pmatrix} \tag{A2}$$

(c) Calculation of angle of incidence

The incident light propagation direction is given by the normalized wave vector $\vec{k} = \begin{pmatrix} 0 \\ 0 \\ -1 \end{pmatrix}$. The angle of incidence φ of light onto any area element may therefore be easily calculated from the scalar product $-\vec{k} \cdot \vec{n} = \cos\varphi$ to give

$$\cos\varphi = \frac{1}{\sqrt{W_x'^2 + W_y'^2 + 1}}. \tag{A3}$$

We note that φ is usually a very small angle $< 1°$ for the window problem since the sag is much smaller than the window dimension.

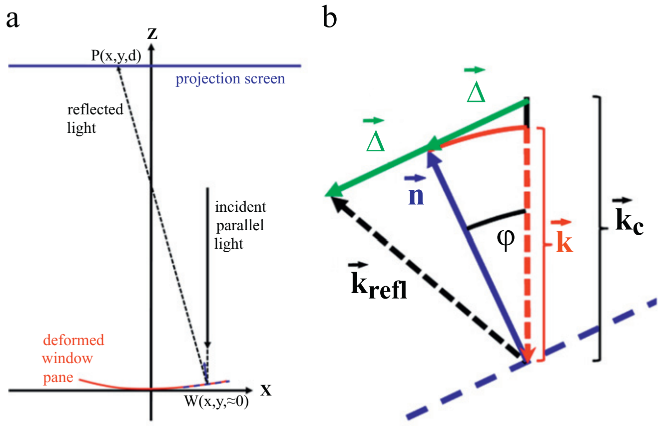

Figure A2. (a) Overview of reflection geometry; (b) directions of unit wave vector $\vec{k}$, unit normal vector $\vec{n}$, respective angle φ as well as magnified vector $\vec{k}_c$ and $\vec{k}_{\mathrm{refl}}$ such that deflection vector $\vec{\Delta}$ is perpendicular to $\vec{n}$.

(d) Calculation of position of reflected light on a projection screen

Figure A2(a) schematically depicts the geometry. Incident light (direction characterized by $\vec{k}$) impinges onto the deformed surface at point $W(x_{\mathrm{win}}, y_{\mathrm{win}}, z_{\mathrm{win}})$. From each area element it is reflected in the direction $\vec{k}_{\mathrm{refl}}$ according to the law of reflection. Its interception with a projection plane, located in a distance $d = z_{\mathrm{screen}}$ from the reflecting window defines the projection spot $P(x_{\mathrm{refl}}, y_{\mathrm{refl}})$. Figure A2(b) depicts the reflection process in term of the relevant unit vectors $\vec{k}$ and $\vec{n}$. Using the known angle (equation (A3)), we define the length C of vector $\vec{k}_c$ as

$$C = \left| \vec{k}_c \right| = \sqrt{W_x'^2 + W_y'^2 + 1} \tag{A4}$$

such that the deflection vector $\vec{\Delta}$ is perpendicular to $\vec{n}$.

Therefore the reflected wave vector is given by $\vec{k}_{\mathrm{refl}} = -\vec{k}_c + 2\vec{\Delta}$. Using $\vec{\Delta} = \vec{k}_c + \vec{n}$ we find

$$\vec{k}_{\mathrm{refl}} = \vec{k}_c + 2\vec{n} = \begin{pmatrix} 0 \\ 0 \\ -C \end{pmatrix} + \frac{2}{C} \begin{pmatrix} -W_x' \\ -W_y' \\ 1 \end{pmatrix}. \tag{A5}$$

The problem now consists in finding the interception of the straight line from the window in direction of the reflected light with the projection plane, i.e. we need to solve

$$\begin{pmatrix} x_{\mathrm{win}} \\ y_{\mathrm{win}} \\ z_{\mathrm{win}} \end{pmatrix} + \lambda \vec{k}_{\mathrm{refl}} = \begin{pmatrix} x_{\mathrm{refl}} \\ y_{\mathrm{refl}} \\ z_{\mathrm{screen}} \end{pmatrix}. \tag{A6}$$

The fixed distance, i.e. the parameter z_{screen} gives λ and therefore the x and y components. Using the approximation that the square root is essentially unity, i.e. $C \approx 1$, we find $\lambda \approx (z_{\mathrm{screen}} - z_{\mathrm{win}}) = d$ which finally gives

$$x_{\mathrm{refl}}(x, y) = x - 2d\frac{\partial W(x, y)}{\partial x} \tag{A7a}$$

and

$$y_{\mathrm{refl}}(x, y) = y - 2d\frac{\partial W(x, y)}{\partial y}. \tag{A7b}$$

Due to the sign change of the partial derivatives when changing from concave to convex mirrors, these equations are valid for either geometry.

References

[1] Lowry C D 1941 Double glazed window *US Patent* 2 228 358

[2] Arici M and Karabay H 2010 Determination of optimum thickness in double-glazed windows for the climatic regions of Turkey *Energy Build.* **42** 1773–8

[3] Cuzzillo B R and Pagni P J 1998 Thermal breakage of double pane glazing by fire *J. Fire Prot. Eng.* **9/1** 1–11

[4] Karlsson J 2001 *Windows Optical Performance and Energy Efficiency* Acta Universitatis Upsaliensis, Comprehensive Summaries of Uppsala Dissertations from the Faculty of Science and Technology 666 Uppsala, available from www.diva-portal.org/smash/get/diva2:161001/FULLTEXT01.pdf

[5] Meyer J 2004 Window for an aircraft with a pressurized cabin (owner airbus Germany) *European Patent EP* 0 846 616 B1

[6] Vollmer M and Möllmann K-P 2012 Caustic effects due to sunlight reflections from skyscrapers: simulations and experiments *Eur. J. Phys.* **33** 1429–55

[7] Schlichting H J 2004 *Lichtkreuze in Lichtkreisen* Der mathematische und naturwissenschaftliche Unterricht (MNU) **57/8** 467–74

[8] Schlichting H J 2006 Reflections on reflections—from optical everyday life phenomena to physical awareness *Informal Learning and Public Understanding* ed G Planinsic and A Mohoric (Ljubljana: University Press) pp 40–52

[9] ABC news 09/30/2010 http://abcnews.go.com/GMA/video/vegas-hotel.window-hazard-exposed-11764297

[10] Hecht E 2002 *Optics* 4th edn (Reading, MA: Addison-Wesley)

[11] Swindell W 1972 Effect of environmental changes on the ghosting of distant objects in twin-glazed windows *Appl. Opt.* **11/9** 2033–6

[12] Filonenko-Borodich M 1963 *Theory of Elasticity* (Moscow: Peace) translation of Russian ed. of 1885; see also online at the Internet Archive https://archive.org/details/theoryofelastcit031768mbp

[13] Smith D J 2000 Flexural stress in windows during hurricanes *Phys. Teach.* **38** 400–2

[14] Wennmacher S 2003 *German State Examination Work for Physics Teachers: Physikalische Untersuchungen zu Reflexionen und Brechungen an gewölbten Oberflächen mit schulischen Mitteln* (Universität Münster)

[15] Vollmer M and Möllmann K-P 2010 *Infrared Thermal Imaging: Fundamentals, Research and Applications* (New York: Wiley)

[16] Möllmann K-P and Vollmer M 2007 Infrared thermal imaging as a tool in university physics education *Eur. J. Phys.* **28** S37–50